AD-A093 813 NAVAL RESEARCH LAB WASHINGTON DC F/G 8/3
DISTORTION OF INTERNAL WAVE PATTERNS BY BACKGROUND SHEAR: A CAS--ETC(U)
DEC 79 T H BELL
UNCLASSIFIED NRL-8362 NL

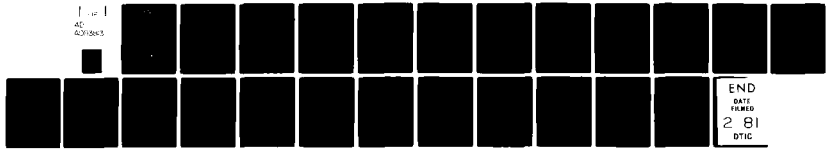

NRL Report 8362

Distortion of Internal Wave Patterns by Background Shear: A Case Study

THOMAS H. BELL, JR.

Applied Oceanography Branch
Ocean Sciences Division

December 26, 1979

NAVAL RESEARCH LABORATORY
Washington, D.C.

14 NRL-8362 16 T1527 17 ZF5955404

SECURITY CLASSIFICATION OF THIS PAGE (When Data Entered)

REPORT DOCUMENTATION PAGE	READ INSTRUCTIONS BEFORE COMPLETING FORM
1. REPORT NUMBER: NRL Report 8362	2. GOVT ACCESSION NO.: AD-A093813
3. RECIPIENT'S CATALOG NUMBER	
4. TITLE (and Subtitle): DISTORTION OF INTERNAL WAVE PATTERNS BY BACKGROUND SHEAR: A CASE STUDY	5. TYPE OF REPORT & PERIOD COVERED: An interim report on a continuing NRL problem.
	6. PERFORMING ORG. REPORT NUMBER
7. AUTHOR(s): Thomas H. Bell, Jr.	8. CONTRACT OR GRANT NUMBER(s): ZF 59-557-004
9. PERFORMING ORGANIZATION NAME AND ADDRESS: Naval Research Laboratory, Washington, D.C. 20375	10. PROGRAM ELEMENT, PROJECT, TASK AREA & WORK UNIT NUMBERS: NRL Problem 83-1103-0
11. CONTROLLING OFFICE NAME AND ADDRESS: Department of the Navy, Naval Material Command, Washington, D.C.	12. REPORT DATE: December 1979
	13. NUMBER OF PAGES: 23
14. MONITORING AGENCY NAME & ADDRESS (if different from Controlling Office)	15. SECURITY CLASS. (of this report): UNCLASSIFIED
	15a. DECLASSIFICATION/DOWNGRADING SCHEDULE

16. DISTRIBUTION STATEMENT (of this Report)

Approved for public release; distribution unlimited.

17. DISTRIBUTION STATEMENT (of the abstract entered in Block 20, if different from Report)

18. SUPPLEMENTARY NOTES

19. KEY WORDS (Continue on reverse side if necessary and identify by block number)

Internal waves
Shear effects

20. ABSTRACT (Continue on reverse side if necessary and identify by block number)

This report constitutes a preliminary comparative study of the structure of numerically simulated internal wave patterns with and without background shear. The analysis focuses on two distinct aspects of the wave pattern: the energy envelope (that region of space within which appreciable density perturbations occur); and the phase information (the structure of the density perturbations within the energy envelope). Using real background oceanographic data, we examine how the energy envelope and phase information observed in the absence of shear are distorted by the presence of background shear. The relevant parameter for determining the relative importance of the

(Continued)

251950

20. Abstract (Continued)

background shear is shown to be the bulk, rather than local, Richardson number, defined in terms of characteristic density and velocity variations over the characteristic dimensions of the wave pattern, rather than in terms of local derivatives of the background density and velocity profiles. Because of the influence of the larger scale, averaged properties of the shear profile on the wave propagation process, the net drift velocity of the energy envelope at any depth level does not accurately reflect the background current speed at that level. Sheer induced restrictions of the vertical extent of the energy envelope are shown to be consistent with elementary wave propagation arguments relating to the so-called critical layer phenomenon. Insofar as the phase information is concerned, we find significant coherence losses (relative to unsheared patterns) over several Brunt-Väisälä periods.

CONTENTS

INTRODUCTION 1

THE WAVE PATTERN 3

DISTORTION OF THE ENERGY ENVELOPE 10

PHASE DISTORTION 13

DISCUSSION 18

REFERENCES 20

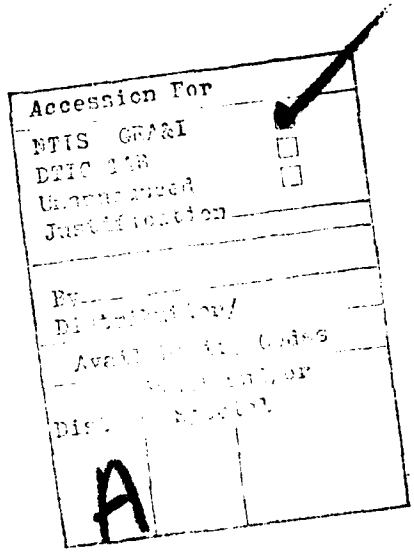

DISTORTION OF INTERNAL WAVE PATTERNS BY BACKGROUND SHEAR: A CASE STUDY

INTRODUCTION

Sheared background currents are known to exert a profound influence on the structure and evolution of internal wave patterns in density stratified fluid systems such as the upper ocean [1]. This report constitutes a preliminary comparative study of the structure of numerically simulated internal wave patterns with and without background shear. The approach adopted in this preliminary study is a phenomenological one. It is basically an exercise in extracting information on shear effects from "pictures" of the internal wave patterns. The purpose of the study is to provide some fundamental quantitative information on the distortion of internal wave patterns in a realistic upper ocean environment. For purposes of analysis, we identify two distinct aspects of the wave patterns: the "energy envelope" and the phase structure within that envelope. The energy envelope is loosely defined as that region of space within which appreciable wave induced density perturbations occur, and the phase structure or information relates to the detailed structure of the density perturbations within the energy envelope.

The numerical simulations described in this report were performed by G. O. Roberts and colleagues at Science Applications, Inc., under contract to the Naval Research Laboratory. The simulations are implemented by the computer code GORWAK, which is described in [2]. The GORWAK code computes finite difference solutions for initial value problems in stratified shear flows. The primary output of the code is maps of stream function, vorticity, and density perturbations associated with the internal wave pattern at selected time steps. This report comprises the results of a comparative study of the structure of the internal wave patterns as revealed by the density perturbation maps with and without background shear. The emphasis is on how certain characteristic features of the internal wave pattern observed in the absence of shear are distorted by the presence of background shear.

Measurements of density and current structure in spring 1973 in the Sargasso Sea area of the western North Atlantic made by T. Sanford and colleagues at the Woods Hole Oceanographic Institution using Sanford's free-fall Electro-Magnetic Velocity Profiler [3] are considered to be representative of typical upper ocean conditions. Profiles of Brunt-Väisälä frequency and background current based on Sanford's data are illustrated in Fig. 1 along with the Richardson number profile. The Brunt-Väisälä frequency (N) is defined in terms of the local vertical density gradient by

$$N^2(z) = -\frac{g}{\rho}\frac{d\rho}{dz}$$

where g is the acceleration of gravity. Background current speed is denoted by $U(z)$ and the local Richardson number is defined as

Manuscript submitted June 26, 1979.

$$Ri(z) = \frac{N^2(z)}{(dU/dz)^2}$$

The profiles in Fig. 1 were used as input environmental data for the computer runs analyzed here. Note that the depth scale in Fig. 1 is relative, rather than absolute. The reference level of 0 m in Fig. 1 corresponds to an actual depth of 80 m in the original data, that is, the profiles in Fig. 1 cover an absolute depth range from 80 m to 280 m. This places the vertical aperture below the seasonal thermocline, in a region where shear effects can be studied without the added complexity which is introduced by large variations in the Brunt-Väisälä frequency profile.

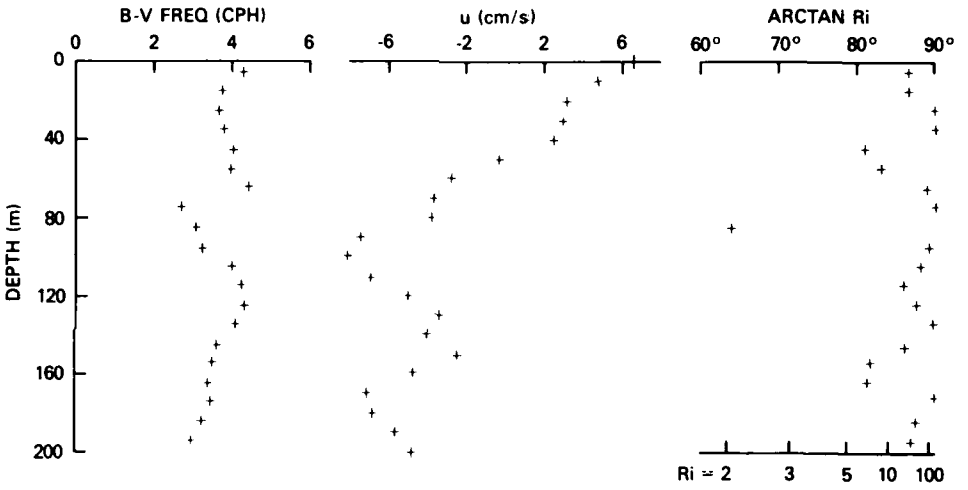

Fig. 1 — Profiles of Brunt-Väisälä frequency and background current speed used in the simulations. Data is taken from actual measurements made by Sanford [3] in the Western North Atlantic. Richardson number profile is shown on the right.

The variability in N and U illustrated in Fig. 1 is probably the combined result of mesoscale and low frequency internal wave motions, so that we may expect associated horizontal variability on scales of order 100 times the scales that characterize the vertical variability. In order to avoid questions relating to the effects of horizontal variability on internal wave propagation, we restrict attention to high frequency internal wave patterns, which are characterized by comparable vertical and horizontal scales. The computer runs analyzed here are then simulations of the response of the upper ocean to a localized input of vertical momentum in the form of an upwardly directed impulsive force, since such forcing is well "tuned" to the generation of high frequency internal waves. The characteristic length scale of the source function was chosen to be 10 m, consistent with the vertical resolution in Sanford's profiles. The calculations were performed in a 200 m by 650 m rectangular grid with absorbing sidewall boundaries and reflecting upper and lower boundaries.

As noted above, the purpose of this study is to provide some fundamental quantitative information on the distortion of internal wave patterns in a realistic upper ocean environment. In the following section, we describe the numerical simulations in more detail and present a sequence of density perturbation maps at various time steps, illustrating the evolution of the internal wave pattern with and without background shear. The next two sections contain the results of a comparative study of the internal wave patterns revealed in the density perturbation maps. The analysis focuses on three primary characteristics of the shear induced distortion of the internal wave patterns: depth dependent advection of the overall pattern by the sheared background currents, the effects of the background shear on the vertical spread of the internal wave pattern, and loss of coherence of the internal structure of the advected pattern relative to the unsheared pattern. The first two effects relate to the distortion of the energy envelope, that is, the shape and size of that region of space within which appreciable density perturbations are found. The third effect relates to shear induced transformations of the phase information or structure within the energy envelope.

Finally, the results are discussed. The primary conclusions are not entirely unanticipated. The results of this study indicate that shear induced distortions in general are primarily related to variations in the background velocity field over vertical scales comparable to the vertical extent of the wave pattern, although precise details of the phase structure in the wave pattern may be influenced by smaller scale variations in the background velocity (and density) fields. Insofar as the evolution of the wave pattern is concerned, two distinct time scales arise. The pattern as a whole expands at a rate determined by the buoyancy time scale (Brunt-Väisälä frequency), while distortion of the phase information proceeds at a rate determined by the background vorticity or shear time scale. The relevant parameter for determining the relative importance of the background shear is the bulk, rather than local, Richardson number, defined in terms of characteristic density and velocity variations over the characteristic dimensions of the wave pattern, rather than in terms of local derivatives of the background density and velocity profiles. For the representative oceanographic conditions considered here, we find that significant coherence losses in the phase structure of the wave patterns (relative to the unsheared wave patterns) occur by the time the patterns are several Brunt-Väisälä periods old, and that shear may significantly inhibit the vertical spread of the wave pattern. A typical situation in which the background velocity varies more or less monotonically with depth, with a characteristic Richardson number of about 20, could effectively confine the sensible internal wave pattern to an overall vertical extent of about 100 m.

THE WAVE PATTERN

The numerical simulations described here were performed under contract to the Naval Research Laboratory by G. O. Roberts of Science Applications, Inc., using Roberts' computer code GORWAK, described in [2]. The background density and current fields used in the calculations were derived from real upper ocean data (Fig. 1). The density and transverse velocity were specified at 10-m depth intervals, down to 200 m. These were interpolated using a cubic spline, and smoothed using a diffusion technique; the smoothing was minimal. The computational domain corresponds to a horizontal range of $-324\text{ m} < y < 324\text{ m}$, and a depth range of 200 m. The displayed domain for the shaded contour diagrams of stream function, vorticity, and density perturbation is square, with horizontal range of $|y| \leqslant 100$ m

and vertical range of $|z| \leqslant 100$ m. Only the contour diagrams of density perturbation are described here. In the calculations, "porous damping" was used in the side regions to avoid any reflection effects from the computational boundaries. Reflections from the top and bottom of the computational domain do appear at the later time steps. The initial disturbance is centered at $y = 0, z = 0$, and has the form

$$\omega = pye^{-\frac{r^2}{a^2}}$$

where ω is the vorticity. The characteristic scale of the disturbance, a, is 10 m, and p was chosen to give an upward momentum impulse of

$$\omega y dA = 2\ m^3/\text{s}.$$

This particular value was chosen to insure that essentially linear dynamics prevail insofar as the forcing function is concerned. Although the GORWAK code is fully capable of dealing with strongly nonlinear phenomena, it was felt that the effects of significant nonlinearity in the forcing function might overshadow some of the effects of the background environment on the wave patterns. The computational mesh spacing was 3.75 m at the disturbance center, and the code ran for a simulated time of 41 min or slightly less than 2½ Brunt-Väisälä periods. Contour diagrams were displayed at roughly 5-min intervals.

The graphic output of the code of interest here are two-dimensional line printer "shadow" plots of the density perturbation associated with the evolving internal wave pattern. The appropriate plots are illustrated in Figs. 2a through 2h. Each figure shows a pair of plots corresponding to the specified elapsed time for calculations corresponding to the Brunt-Väisälä frequency profile illustrated in Fig. 1. The nondimensional times (NT) are based on a representative Brunt-Väisälä frequency of $6 \times 10^{-3}\ \text{s}^{-1}$. The plots on the left hand side of each figure correspond to calculations run with no background currents, and those on the right include the effects of the background velocity profile shown in Fig. 1. Figures 2a through 2h illustrate the evolution of the wave pattern with and without realistic background shear. The shadow patterns in the plots are produced by numerals, letters, and overprints. Numerals correspond to positive density perturbations, and letters to negative ones. The actual characters (poorly resolved in the reduced plots illustrated here) are related to the magnitude of the density perturbation. However, in this study, we are not concerned with the magnitudes of the density perturbations, but rather with the shape and structure of the patterns as revealed by the shadow plots.

There is no plot for time $t = 0$, since the internal wave field is generated by an impulsive force, corresponding to an initial condition on the velocity, rather than density field. The initial density perturbation is zero, but the initial time rate of change of the density perturbation, which is related to the initial velocity field, is nonzero.

The complexity of the internal wave patterns increases with increasing time. This is manifested by the appearance of more and more "lobes" or "fingers" with the passage of

time. The fingers are simply manifestations of the number of oscillations within the pattern, which increases with time as the wave field evolves. The lack of symmetry in the unsheared patterns is a result of the nonuniform background density stratification. The Brunt-Väisälä frequency above the centerline is somewhat less than below. With background currents included (right-hand panels), the up-down asymmetry is especially pronounced. Again, this is a direct result of the differences in the environment above and below the centerline. Although there is considerable structure within the velocity profile, the net shear above the centerline is significantly greater than the net shear below the centerline.

Qualitative characteristics of the dominant shear effects are obvious in Figs. 2a through 2h. For purposes of analysis, we recognize two distinct properties of the wave pattern. The first is the "energy envelope," loosely defined as that region of space within which appreciable wave induced density perturbations occur. The second is the phase structure or information which relates to the detailed structure of the density perturbations within the energy envelope. With regards to the energy envelope, it is clear that the wave pattern is being locally advected by the prevailing currents. It is also apparent that the vertical spread of the pattern is significantly inhibited by the shear. The internal structure of the patterns is also affected by the shear. Even taking into consideration the gross advective distortion of the patterns, certain features of the internal structure of the patterns are destroyed or severely distorted by the background shear. In the next two sections, these shear-induced distortions are described in detail, and parameterized in terms of gross characteristics of the background velocity profile.

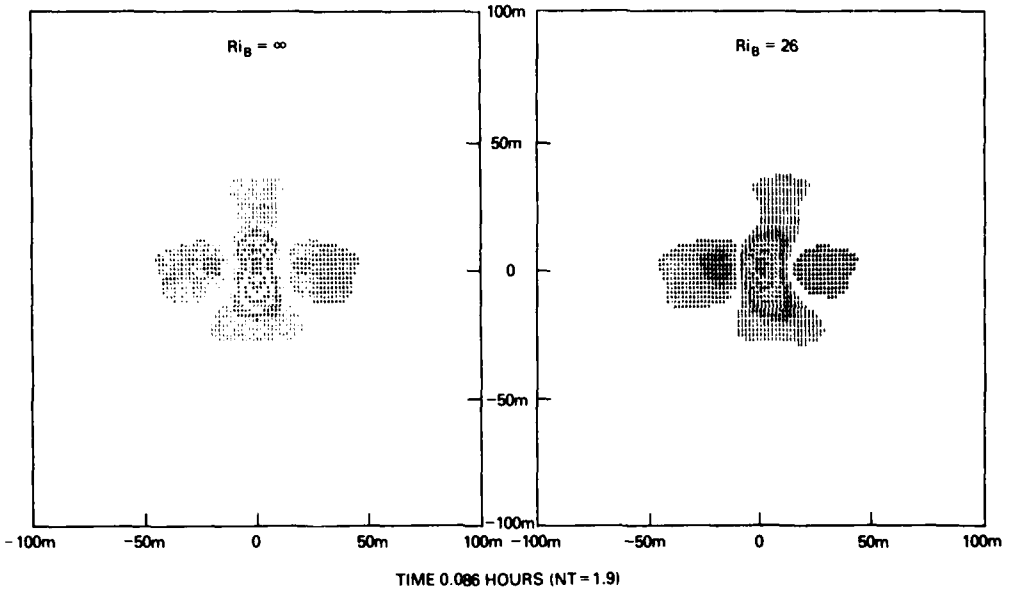

Fig. 2a — Shadow plot of density perturbation associated with evolving internal wave pattern at time 0.086 h after generation. NT is nondimensional time based on representative Brunt Väisälä frequency 6×10^{-3} s^{-1}. Viewing plane is vertical slice of similated ocean 200 m high by 200 m wide. Shear free case ($Ri_B = \infty$) on left, sheared case ($Ri_B = 26$) on right.

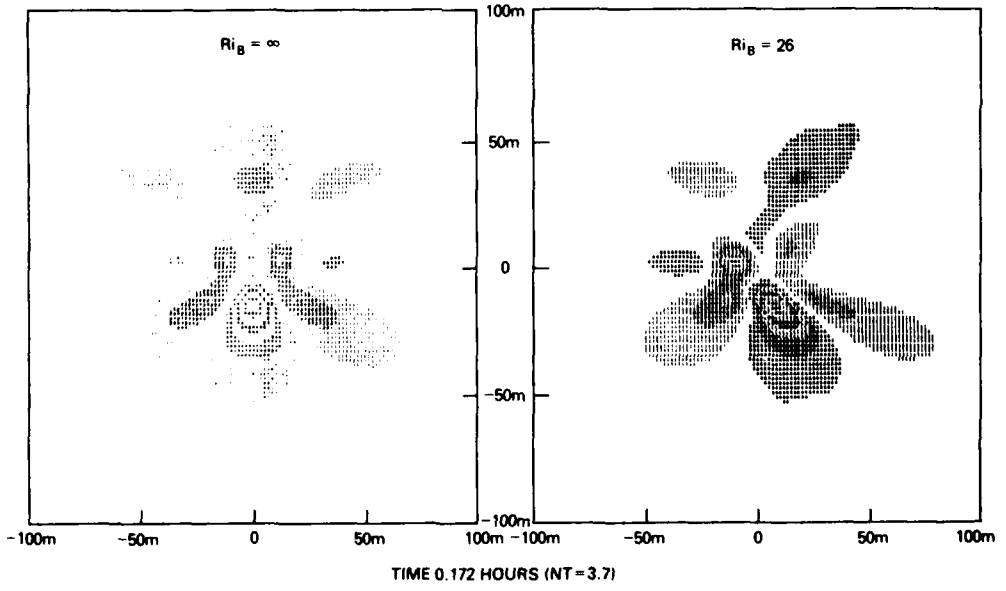

Fig. 2b — Same as 2a for evolution time of 0.172 h

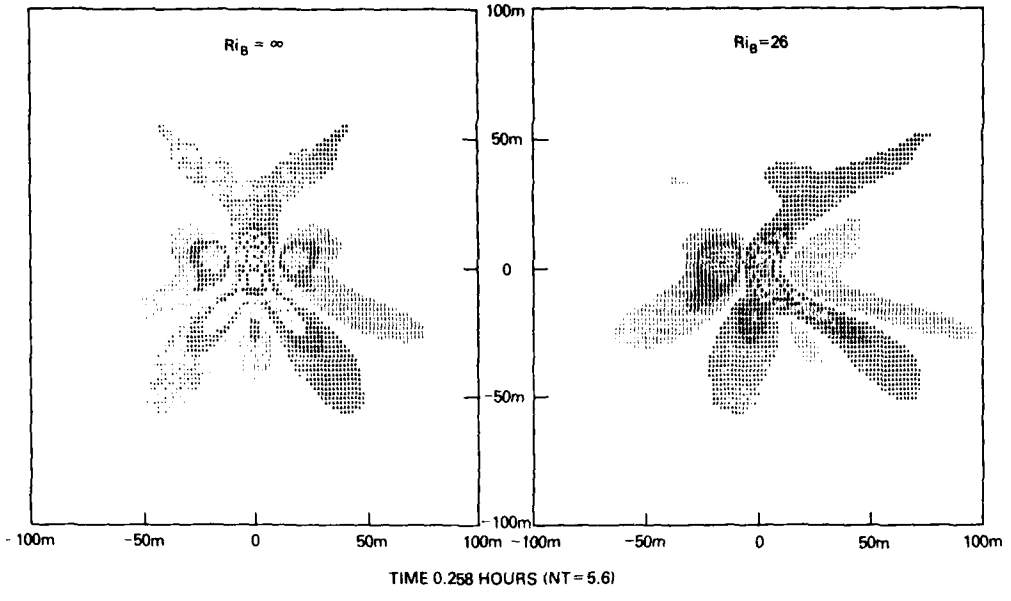

Fig. 2c — Same as 2a for evolution time of 0.258 h

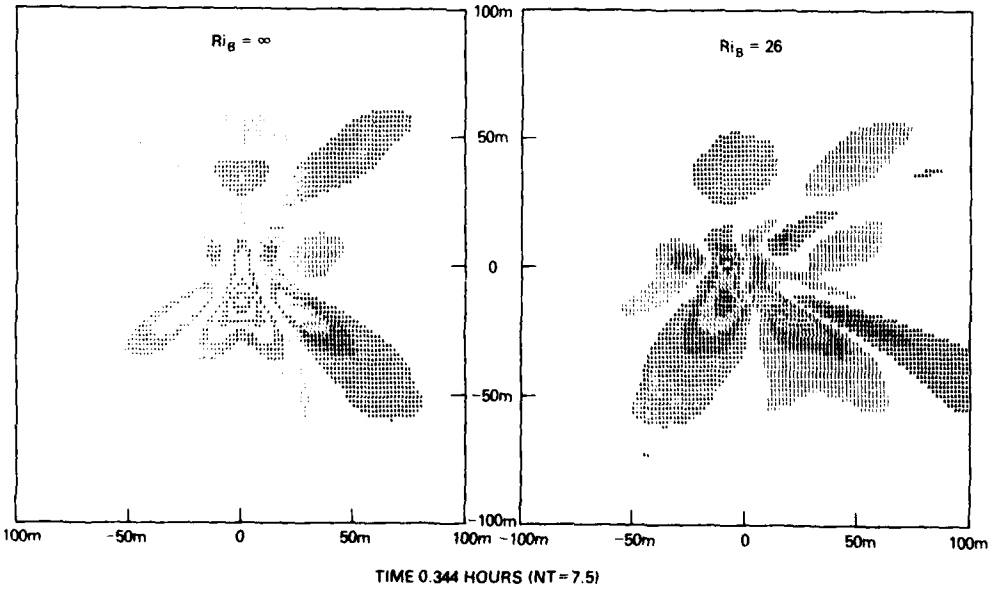

Fig. 2d — Same as 2a for evolution time of 0.344 h

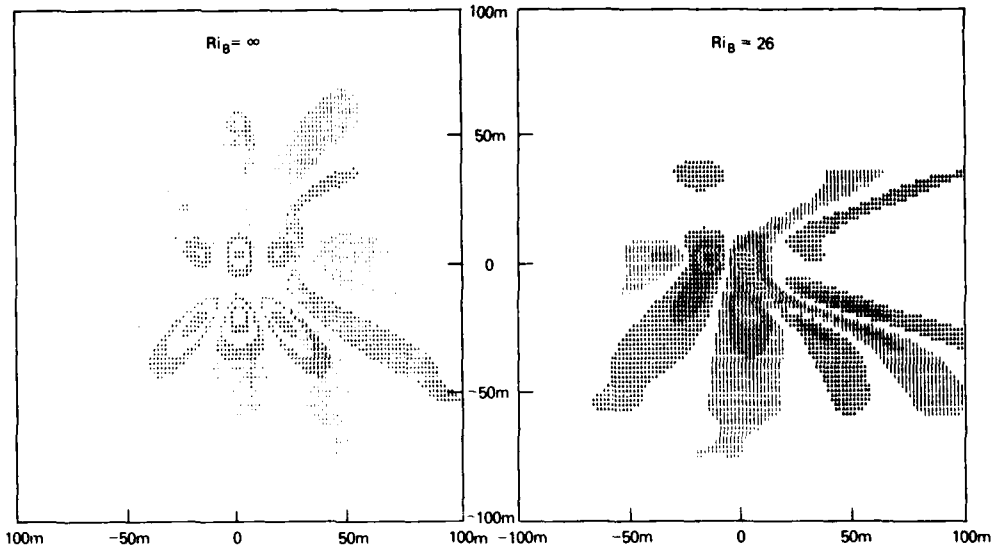

Fig. 2e — Same as 2a for evolution time of 0.430 h

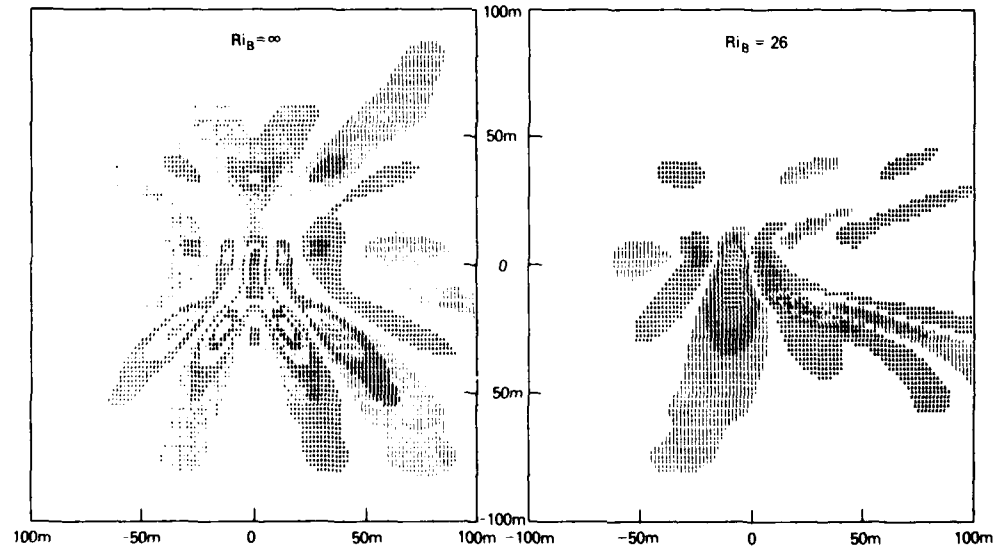

Fig. 2f — Same as 2a for evolution time of 0.516 h

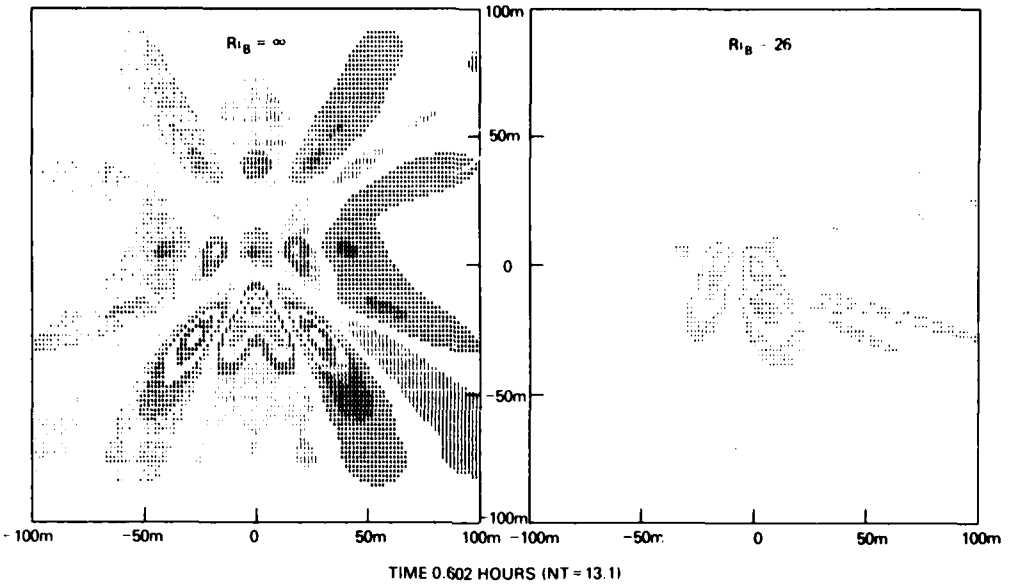

Fig. 2g — Same as 2a for evolution time of 0.602 h

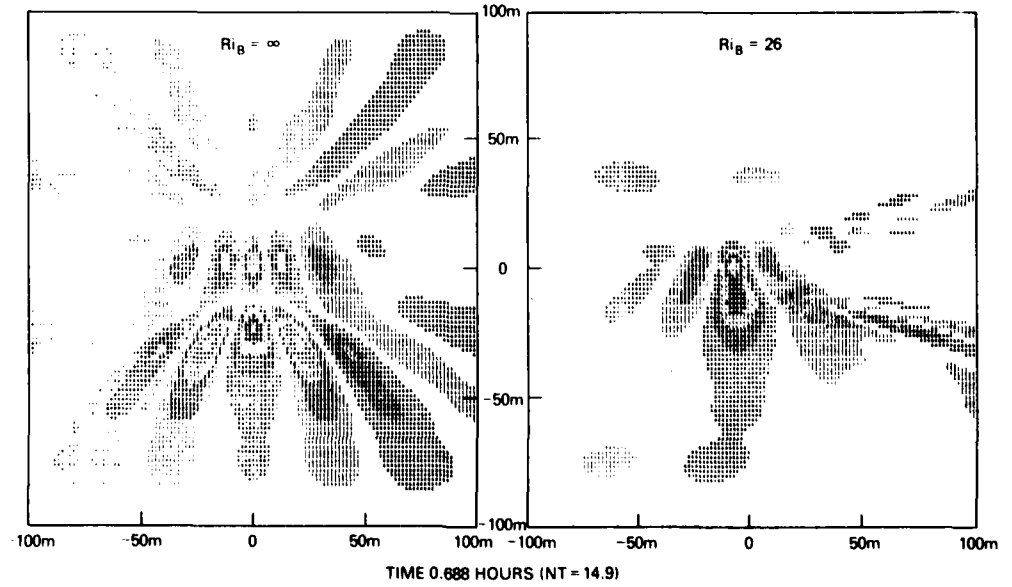

Fig. 2h — Same as 2a for evolution time of 0.688 h

DISTORTION OF THE ENERGY ENVELOPE

As noted above, the most obvious effect of the background current field is advective. The wave pattern appears to be carried along by the prevailing background currents. In the unsheared case (left-hand panels in Fig. 2), the evolving pattern remains centered on $y = 0$, and retains a left-right symmetry. This is not the case when sheared background currents are included. At each depth level, the pattern drifts farther and farther from the centerline ($y = 0$) with the passage of time. Data relating to this advective distortion of the wave pattern is plotted in Fig. 3. The individual data points in Fig. 3 represent apparent relative drift velocities of the pattern at various depth levels. Relative velocities are referenced to the centerline depth (100 m), which corresponds to the vertical coordinate $z = 0$. At any depth level, individual points represent estimates of the apparent net drift velocity at different evolution times. Because the data is rather sparse and somewhat scattered, it was not possible to isolate any systematic dependence of apparent drift velocity on evolution time. It is likely, however, that such a relationship may exist, tending towards some asymptotic limit for very late times. The solid curve in Fig. 3 is the background relative velocity profile. Since the data does not cluster about the relative velocity profile, it is clear that we are not dealing with a purely local advective phenomenon. Rather, the net drift of the pattern is a composite of local advection combined with dispersive wave propagation effects which are influenced by the background shear flow.

The dashed line in Fig. 3 is a smoothed velocity profile $\overline{U}(z)$, such that

$$\overline{U}(z) = \frac{1}{z} \int_0^z [U(z) - U(0)]\, dz,$$

that is, it is the average relative velocity over the depth range from the vertical centerline ($z = 0$) to the depth level of interest. This represents a very simple transformation of the relative velocity profile that recognizes the fact that the wave propagation depends on the overall shear profile, especially that portion of the profile between the depth level at which measurements are made and the depth at which the wave pattern was generated. Below the centerline, the data points appear to correlate more with the averaged velocity profile than the centerline; the two profiles appear to bracket the data. This difference above and below the centerline appears to be related to the fundamentally different nature of the background velocity above and below the centerline. Above the centerline, the relative velocity continuously increases with height above the centerline. Simple wave propagation arguments (see [1], for example) indicate that in such an environment, the wave energy is trapped by the background velocity field, which acts as a potential barrier to wave propagation. The nature of this trapping is such that the group velocities of the various wave components asymptotically approach the local background current speed. Below the centerline, the velocity profile is not monotonic, and wave energy is able to penetrate through the local extrema in the profile. Hence, we expect that the apparent drift velocities below the centerline will be more dependent on the averaged velocity profile than those above the centerline, which will in turn be more closely related to the relative velocity profile itself.

It should be stressed that the process of internal wave propagation in a shear flow is a complex one, and that the precise details of the local drift of the energy envelope are in fact

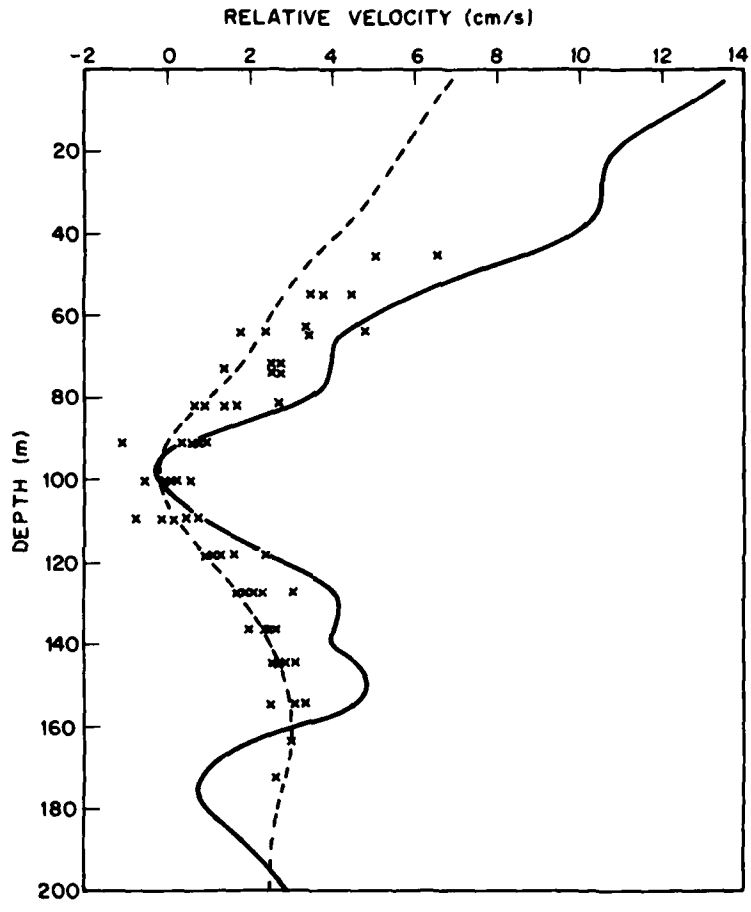

Fig. 3 — Apparent relative drift velocity of internal wave pattern as a function of depth (x's). Solid line is background relative velocity profile. Dashed line is average relative velocity between any depth and source depth of 100 m.

a functional of the entire density and background velocity profiles. The fact that the apparent drift velocities seen here seem to be bounded by the relative velocity profile and an appropriately smoothed version of that profile is basically an empirical observation. It indicates that the net displacement of the wave pattern by the background currents is not a purely advective phenomenon, but also depends on larger scale averaged properties of the background shear field.

As noted above, an examination of Figs. 2a through 2h reveals that sheared background currents tend to inhibit the vertical spread of the wave pattern. Data on the vertical spread of the wave pattern as a function of time is presented in Fig. 4. Vertical extent of the wave pattern is measured directly from Figs. 2a through 2h, and, as such, represents the maximum vertical distance from the centerline ($z = 0$) at which sensible density perturbations are found. Because of the manner in which Figs. 2a through 2h were produced, "sensible density perturbation" is a relative term, meaning density perturbations which are about 15% of the maximum density perturbation associated with the wave pattern. Time is nondimensionalized with an average Brunt-Väisälä period of 16 min. The diagonal dashed lines in Fig. 4 represent a least squares fit to the no-shear data for times less than 2 Brunt-Väisälä periods, and correspond to a vertical spreading rate of 3.2 cm/s. For the forcing function used to generate the wave patterns, the characteristic vertical group velocity or rate of energy propagation should be $\frac{1}{4}\sqrt{\pi}\,Na$, where N is the representative value of the Brunt-Väisälä frequency ($6.6 \times 10^{-3}\ s^{-1}$) and a is the characteristic scale of the disturbance (10 m). Using the characteristic values of N and a, the characteristic group velocity turns out to be 2.9 cm/s, in good agreement with the observed spreading rate.

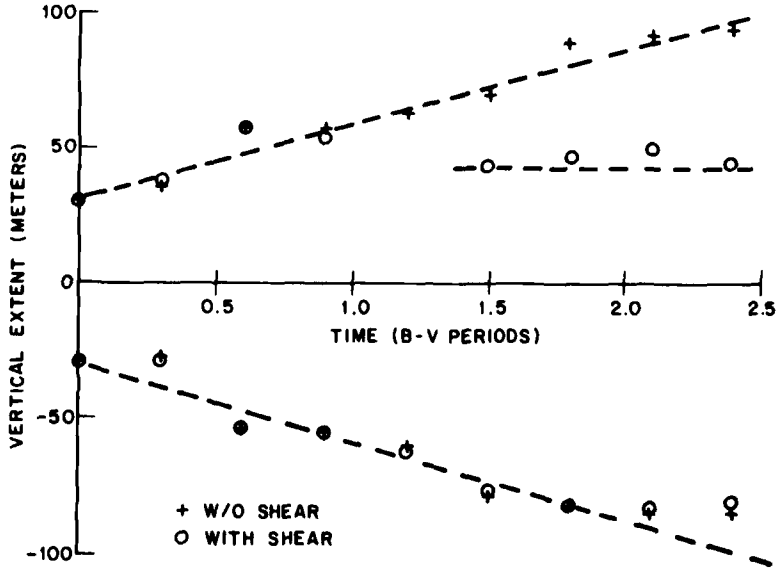

Fig. 4 — Vertical extent of wave patterns as a function of time in Brunt-Väisälä periods. See text for significance of dashed lines.

The no-shear wave patterns tend to flatten out after about 2 Brunt-Väisälä periods. This is due to reflection from the upper and lower boundaries of the computational domain. Below the centerline, the vertical spread of the sheared pattern is virtually identical to that of the unsheared pattern. Above the centerline, the sheared pattern flattens out at a height of 40 or 50 m above the centerline. This is a direct consequence of the monotonic shear above the centerline. As internal wave energy propagates away from the source region, the frequencies of the various component waves are Doppler shifted by the prevailing background currents. Components whose frequency is Doppler shifted up to the local Brunt-Väisälä frequency are reflected back down towards the source level. Because of the superposition of incident and reflected waves, the magnitude of the density perturbations in the vicinity of the reflection regions is generally quite small. Wave components whose frequency is Doppler shifted down to zero frequency can no longer propagate, and are simply advected by the prevailing background currents. It is this latter process (the so-called critical layer phenomenon) that determines the range of depths within which the energy envelope is confined. The characteristic horizontal phase speed of the waves is

$$\frac{1}{2}\sqrt{\pi}\,Na \approx 5.3 \text{ cm/s}.$$

A relative current of about 5.3 cm/s will then Doppler shift the waves to zero frequency. This occurs at a level of about 40 or 50 m above the centerline, as indicated by the horizontal dashed line in Fig. 4. Below the centerline, the background velocity profile is recurved, rather than monotonic. Although the peak relative velocity below the centerline is about 5 cm/s, the fact that the background current speed decreases again below the peak allows a substantial portion of the wave energy to penetrate through the "barrier" created by the peak relative velocity, and hence, we do not see the dramatic flattening of the wave patterns below the centerline. The dramatic difference in vertical spread of the wave pattern above and below the centerline is especially significant in that it emphasizes the importance of the large scale structure of the background velocity profile in determining the effect of shear on the wave patterns.

PHASE DISTORTION

In addition to the depth dependent net displacement of the internal wave pattern by the prevailing currents and the inhibition of vertical spread of the wave patterns, the internal structure of the patterns is affected by the shear. Certain features of the internal structure of the patterns are destroyed or severely distorted. Relative to the unsheared case, the phase information within the sheared wave pattern becomes more and more distorted with the passage of time. In order to quantify this relative loss of phase information, we have concentrated on a comparison of individual features within the patterns in the presence and absence of background shear. The phase information in the patterns is contained in the structure and time evolution of the lobes or fingers that comprise the patterns. Any individual lobe can be followed in time from its origin along the vertical centerline of the pattern, as it propagates outwards through the pattern, until it finally disappears at the edges of the pattern. At any given depth level and time, we may compare the width of a particular lobe as seen with and without background shear. If W_o is the width of the lobe in

the unsheared case and W is the width of the corresponding lobe with background shear included, then we define an angle β such that

$$\tan \beta = W/W_o .$$

Thus, if the width of the lobe is unchanged by the shear, then $\beta = 45^\circ$. If the width is increased by shear, then $\beta > 45^\circ$, and conversely $\beta < 45^\circ$ if the width of the feature is decreased by the shear. A feature which is present in the unsheared case and absent in the sheared case corresponds to $\beta = 0^\circ$, while the opposite case corresponds to $\beta = 90^\circ$. Clearly, values of β near 45° correspond to minimal shear-induced distortion of the individual features which make up the wave patterns, whereas values of β approaching 0° or 90° correspond to maximal shear-induced distortion.

Frequency distributions of measured values of the parameter β described above at various times during the evolution of the wave patterns are illustrated in Fig. 5. A frequency distribution which is tightly clustered about $\beta = 45^\circ$ implies little shear-induced distortion of phase information. Figure 5 shows that as the wave patterns evolve with the passage of time, the frequency distributions broaden, and a systematic bias towards values of β near 0° appears. This is indicative of substantial shear-induced distortion of the phase information in the wave patterns. The increase in values of β near 0° is especially significant since it represents an effective loss of phase information relative to the unsheared case. This loss of information is not compensated for by a significant gain in phase information which would show up as an increase in the frequency of occurrence of β near 90°.

We may parameterize the systematic distortion and loss of phase information by examining the time evolution of the frequency distributions of the parameter β. To this end, we divide the range of values of β into three intervals: 0 to 30°, 30 to 60°, and 60 to 90°. Values of β in the middle interval are indicative of minimal shear-induced distortion, whereas values of β in the outer intervals indicate significant shear-induced distortion in the internal structure of the wave patterns. The upper graph in Fig. 6 shows the relative number of measured values of β in the three intervals as a function of time as the wave patterns evolve. There is a clear systematic decrease in the relative frequency of occurrence of values of β in the range 30 to 60°. This is balanced by an increase primarily in the relative frequency of occurrence of low, rather than high, values of β, which is indicative of a systematic loss, rather than a simple restructuring, of the phase information in the sheared wave patterns relative to the unsheared patterns. The lower graph in Fig. 6 illustrates that the shear-induced distortion proceeds at a significantly faster rate above the centerline of the wave pattern than below. That figure shows the relative number of measured values of β in the middle interval as a function of time for data taken above the centerline at $Z = 0$ and for data below the centerline. The differences may be attributed to the differences in the nature of the background shear profile above and below the centerline of the pattern. Although values of the local Richardson number are comparable above and below the centerline, the gross characteristics of the shear profile are markedly different above and below the centerline.

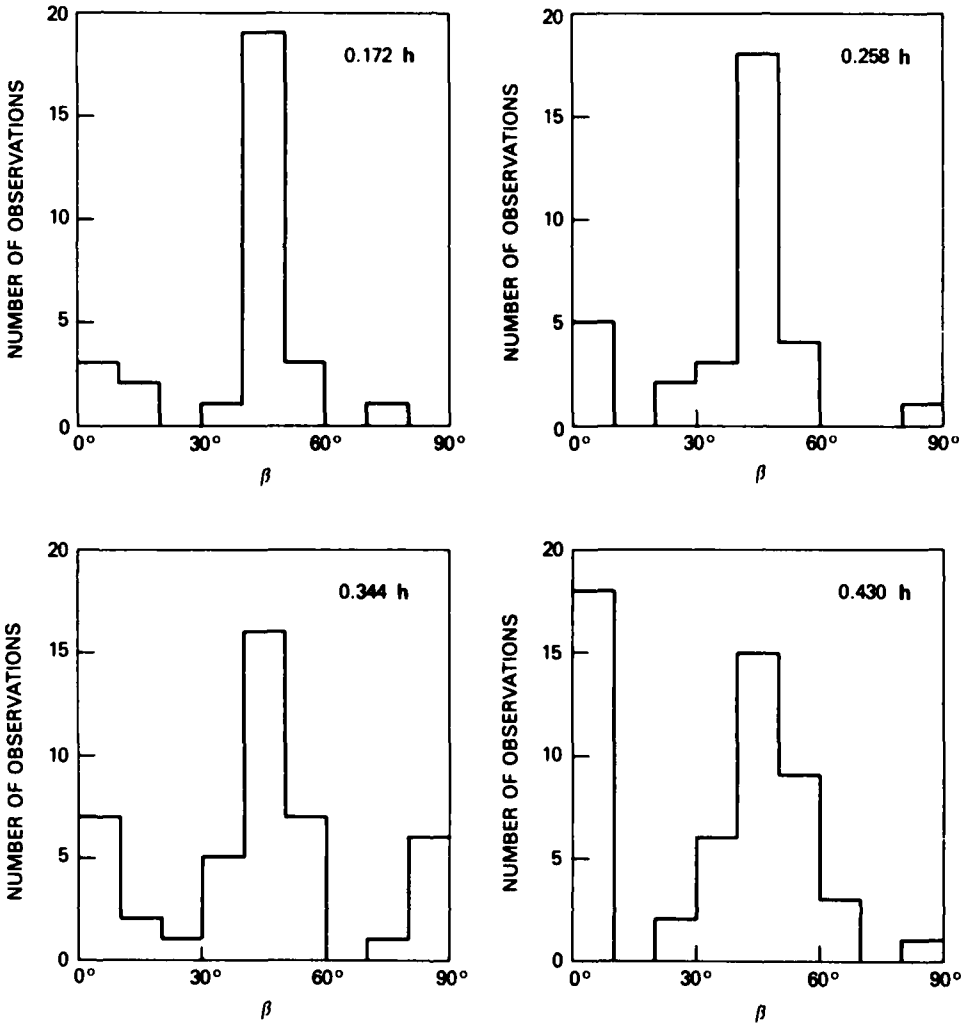

Fig. 5 — Frequency of occurrence histograms of parameter β for sheared wave patterns at various evolution times. β is a measure of the relative distortion of phase information in the sheared wave pattern. Shear induced distortion is minimal for $\beta = 45^{\circ}$ and maximal for $\beta = 0^{\circ}$ or 90°.

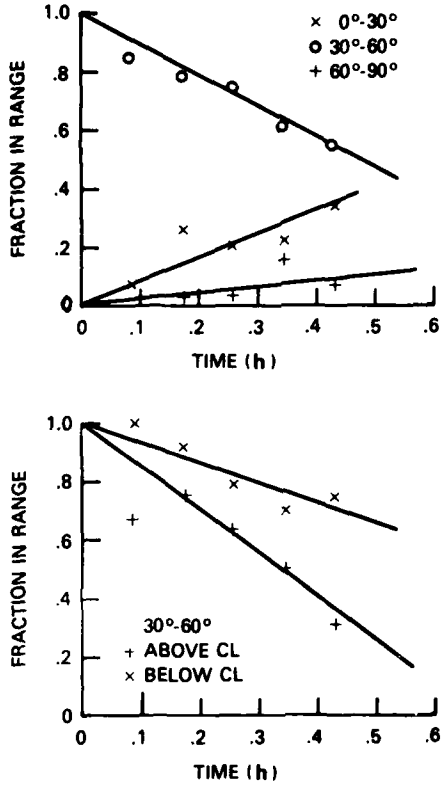

Fig. 6 — Time evolution of frequency distributions of parameter β. Upper frame shows relative frequency of occurrence of values of β in three ranges (0 to 30°, 30 to 60°, 60 to 90°) as a function of time for the entire wave pattern. Lower frame shows frequency of occurrence of β in range 30 to 60° for upper and lower half of wave patterns.

We may loosely parameterize the gross characteristics of the shear profile by introducing a bulk Richardson number Ri_B, defined by

$$Ri_B = \frac{1}{\rho_0} \frac{g\Delta\rho D}{(\Delta U)^2} \ ,$$

where D is a characteristic vertical distance, and $\Delta\rho$ and ΔU are characteristic density and current velocity variations. The definition of bulk Richardson number is intentionally vague. Precisely what is meant by "characteristic" will depend on the particular application of interest. For the case at hand, the characteristic vertical distance clearly relates to the vertical extent of the wave field and $\Delta\rho$ refers to the net change in density over the depth range D. The characteristic velocity scale is a bit more difficult to pin down. In general, ΔU may be taken as the difference between the maximum and minimum background current velocities occurring in the depth range D. An important exception occurs when we have a wave pattern more or less centered on an extremum in the velocity profile, such as is the case here. In such cases, because the wave energy radiates both upwards and downwards, we must choose $\Delta U = \Delta U_u + \Delta U_L$, where ΔU_u and ΔU_L are representative values of ΔU above and below the middle of the pattern. (Note that in this context, we consider ΔU values to be inherently positive, irrespective of whether velocity is increasing or decreasing

with depth.) Characteristic values of the bulk Richardson number for the case at hand turn out to be in the low to mid teens above the centerline, around 50 below the centerline, and in the mid twenties for the entire pattern. This is in direct contrast to the fact that values of the local Richardson number are comparable above and below the centerline. Although the magnitude of the local shear dU/dz is much the same above and below the centerline, the gross characteristics of the velocity profile are different above and below. Hence, the differences between local and bulk Richardson numbers above and below the centerline.

The rate at which the relative frequency of occurrence of values of β in the 30 to 60° range decreases with time is a measure of the rate of shear induced distortion of the phase information in the wave patterns. Referring to Fig. 6, the relative frequency of occurrence of β in the 30 to 60° range decreases more or less linearly with evolution time. If $\mu(t)$ is defined as that relative frequency at time t, then we may define an effective decay time τ by

$$\tau = \frac{t}{1-\mu(t)} .$$

If we extrapolated the 30 to 60° lines in Fig. 6 until they intersected the time axis, τ would be the point of intersection. In Fig. 7, we have plotted effective decay time as a function of bulk Richardson number. There are three sets of points in that figure. Crosses refer to observations above the centerline, x's to points below the centerline, and circles refer to the entire wave field. Each set contains four points, corresponding to the four times for which frequency distributions appear in Fig. 5. In each case, the bulk Richardson number is computed using a vertical scale D equal to the relevant vertical extent of the wave pattern (i.e., either the extent above the centerline, the extent below the centerline, or the overall vertical extent of the pattern). Decay times have been nondimensionalized by the appropriate value of the Brunt-Väisälä period ($2\pi/N$). The scatter in the points appears to be primarily related to the fact that we are dealing with relatively small data samples. There is a clear tendency for decay time to increase with increasing Richardson number. The dashed line in Fig. 7 has a slope of 1/2, suggesting that nondimensional decay time increased as the square root of bulk Richardson number. This is a significant observation, although it is not unanticipated. There are natural time scales associated with the density stratification and the shear. The Richardson number is basically the square of the ratio of these time scales. A large value of the Richardson number means that the shear time scale is large compared to the buoyancy time scale, and vice versa. In Fig. 7, the decay time is nondimensionalized by the Brunt-Väisälä period, i.e., the buoyancy time scale. The fact that the decay time nondimensionalized in this way increases as the square root of Richardson number implies that the decay time is directly proportional to the shear time scale $D/\Delta U$. This is, of course eminently reasonable, since it is the shear which is distorting the phase information. If the dashed line in Fig. 7 is assumed to be a fair representation of the relationship between decay time and shear, then as a rough rule of thumb, we may generally expect that 50% of the phase information in a sheared wave pattern will be significantly distorted (relative to an unsheared pattern) as the pattern evolves during a time interval of about $2D/\Delta U$.

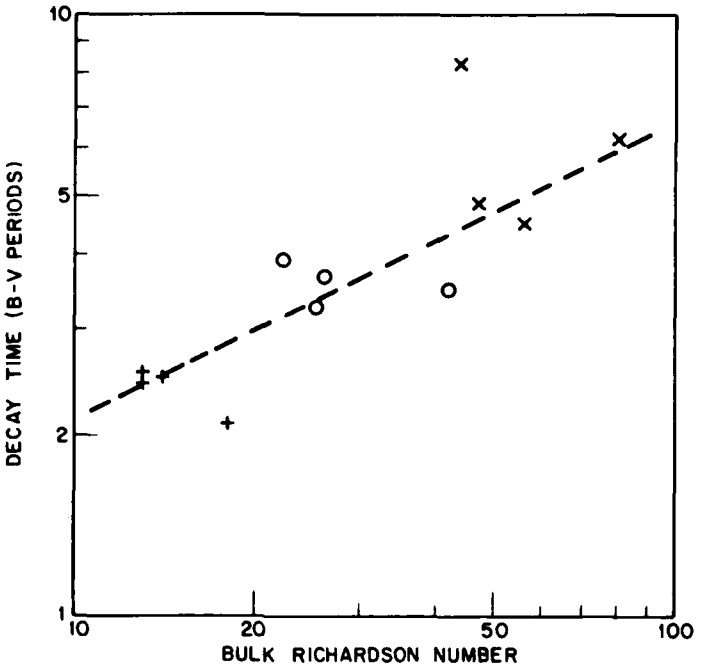

Fig. 7 — Decay time (extrapolated time for no values of β in 30 to 60° range) in Brunt-Väisälä periods as a function of bulk Richardson number. +, upper half of pattern; X, lower half of pattern; O, entire pattern. Dashed curve has slope of 1/2 signifying that decay time is directly proportional to shear time scale ($\sqrt{Ri_B}$ times Brunt-Väisälä period).

DISCUSSION

As noted in the introduction, the purpose of this study is to provide some fundamental quantitative information on the distortion of internal wave patterns by background shear in a realistic upper ocean environment. The analysis focuses on two distinct aspects of the wave pattern: The "energy envelope" and the phase structure within that envelope. The energy envelope is loosely defined as that region of space within which appreciable wave induced density perturbations occur, and the phase structure or information relates to the detailed structure of the density perturbations within the energy envelope.

Shear induced distortion of the energy envelope is twofold. There is a depth dependent advection of the wave pattern by the sheared background currents, and the overall vertical extent of the pattern is limited by the shear. We find that the advective distortion of the energy envelope is not a purely local advective phenomenon. That is, the net drift velocity of the pattern at any depth level is not equal to the relative background current speed at that level. Generally, the local drift velocity is somewhat less than the local current speed.

The net drift of the pattern is a composite of local advection combined with dispersive wave propagation effects which are influenced by the background shear flow, so that the precise details of the local drift of the energy envelope are in fact a functional of the entire density and background velocity profiles. No simple expression of that function dependence exists. However, we do find that in general the net drift at any level lies between the local relative background current speed at that level and the average relative background current speed between the observation level and the source level at which the wave field was generated. The vertical spread of the wave patterns is inhibited in the presence of background shear by wave reflection from the shear profile and by the so-called critical layer phenomenon, in which wave components Doppler shifted down to zero frequency by the background currents cease to propagate, and are simply advected along by the prevailing background currents. If the relative current speed increases monotonically away from the source level, then the wave pattern will generally be confined to that range of depth within which the relative background current speed is less than the characteristic horizontal phase speed of the dominant wave components which make up the disturbance pattern. If the background current profile is not monotone, but recurved, the wave pattern may expand indefinitely, even if local extrema in the relative velocity profile are comparable in magnitude to the characteristic horizontal phase speed of the wave components that make up the disturbance pattern.

Even taking into account the gross advective distortion of the wave patterns by the background shear, certain features of the internal structure of the patterns are destroyed or severely distorted by the background shear. This shear induced phase distortion is shown to proceed at a rate proportional to the gross or bulk shear time scale $D/\Delta U$, where D is the characteristic vertical extent of the wave pattern and ΔU is the range of background current speeds occurring in the depth range D. If the data analyzed here is considered to be representative, then we may generally expect that about 50% of the phase information in a sheared wave pattern will be destroyed or at least significantly distorted (relative to an unsheared pattern) as the pattern evolves during a time interval of about $2D/\Delta U$.

We may draw two significant conclusions from this study. The first relates to the length scales of variation in the background shear profile which are important in determining the shear induced distortion of internal wave patterns arising from localized sources, and the second relates to the time scales for the evolution of the wave pattern. The results of this study indicate that shear induced distortions in general are primarily related to variations in the background velocity field over vertical scales comparable to the vertical extent of the wave pattern, although precise details of the phase structure in the wave pattern may be influenced by smaller scale variations in the background velocity (and density) fields. Insofar as the evolution of the wave pattern is concerned, we find that two distinct time scales are significant. The pattern as a whole, that is, the energy envelope, expands at a rate determined by the buoyancy time scale (Brunt-Väisälä frequency), while distortion of the phase information proceeds at a rate determined by the gross shear time scale. Both time scales are equally important in determining the overall evolution of a wave pattern in any realistic ocean environment. A measure of the relative magnitudes of these two time scales is provided by the bulk Richardson number

$$Ri_B = \frac{1}{\rho_0} \frac{g\Delta\rho D}{(\Delta U)^2}$$

where D is a characteristic vertical distance related to the vertical extent of the wave pattern, and $\Delta\rho$ and ΔU are characteristic density and current velocity variations over D. The bulk Richardson number is the square of the ratio of the shear time scale to the buoyancy time scale. Hence, if the overall wave pattern evolves on a time scale T, distortions of the phase information proceed on a time scale $\sqrt{Ri_B}$ T.

Admittedly, the analysis of shear induced distortions of internal wave patterns presented here is a crude one. The approach taken here has been a phenomenological one, basically an exercise in extracting information on shear effects from "pictures" of the internal wave patterns. The study is by no means comprehensive, and the results should be considered as preliminary, rather than conclusive. A more definitive study should examine a wider range of shear conditions in a systematic manner, and should focus on properties of the wave field which are more precise and objective. In particular, the phenomenological definitions of energy envelope and phase information employed in this preliminary study should be replaced with more objective definitions related to integral properties of the wave field. The energy envelope could be objectively defined in terms of various moments of the density perturbation field (in practice, one might use the magnitude or the square of the density perturbations in calculating the various moments). In a similar fashion, objective measures of the phase structure could be related to moments of the Fourier transform of the density field (again, either in terms of the magnitude or squared magnitude of the Fourier coefficients). Unfortunately, displays such as those included in Fig. 2 are not suitable for extracting such information, hence the phenomenological approach adopted here. However, the relevant integral properties of the wave patterns (including, perhaps, patterns of the perturbation vorticity field or other relevant properties) could be calculated directly before the output stages of the numerical simulations, and further efforts at producing a definitive study of shear induced distortions of internal wave patterns should proceed along such lines.

REFERENCES

1. P.H. LeBlond and L.A. Mysak, "Waves in the Ocean," ELSEVIER (1978).

2. G.O. Roberts and D.M. Rubenstein, "Shear Effects on Internal Gravitational Wave Propagation," Science Applications Inc., Report SAI 80-973-WA, June 1980.

3. T.B. Sanford, R.G. Drever and J.H. Dunlap, "The Design and Performance of a Free-Fall Electro-Magnetic Velocity Profiler," Woods Hole Oceanographic Institution technical report Ref. WH01-74-46 (July 1974).

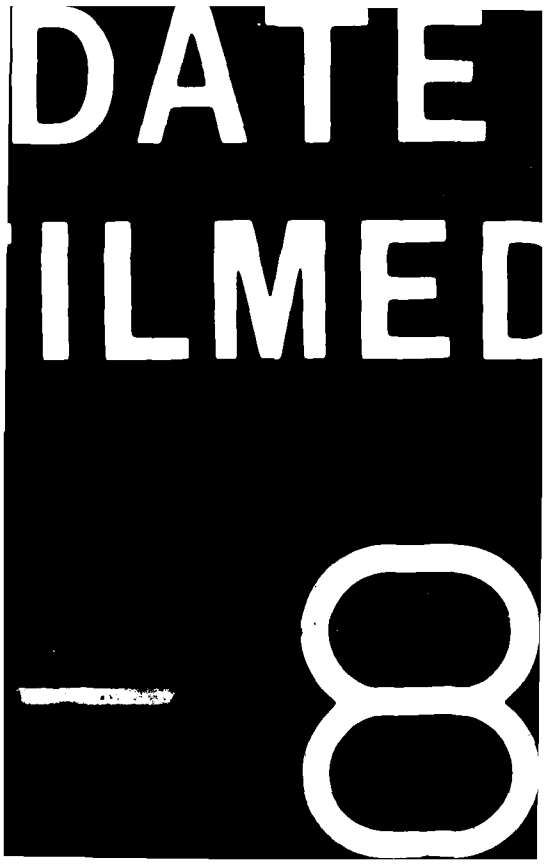
DATE
ILMED
8